

Loops and legs: ABJM amplitudes from f -graphs

Song He,^{a,b,c,d} Yao-Qi Zhang^{a,d,e}

^a*Institute of Theoretical Physics, Chinese Academy of Sciences, Beijing 100190, China*

^b*School of Fundamental Physics and Mathematical Sciences, Hangzhou Institute for Advanced Study and ICTP-AP, UCAS, Hangzhou 310024, China*

^c*Peng Huanwu Center for Fundamental Theory, Hefei 230026, China*

^d*School of Physical Sciences, University of Chinese Academy of Sciences, No.19A Yuquan Road, Beijing 100049, China*

^e*Department of Physics, Astronomy and Mathematics, University of Hertfordshire, Hatfield, Hertfordshire, AL10 9AB, United Kingdom*

E-mail: songhe@itp.ac.cn, y.zhang59@herts.ac.uk

ABSTRACT: We initiate a systematic study on how to extract planar integrands of (super-symmetric) scattering amplitudes with L loops and n legs in Aharony-Bergman-Jafferis-Maldacena (ABJM) theory from the recently proposed (bosonic) generating function for squared amplitudes with $N := n+L$ dual points; the latter enjoys a hidden permutation symmetry S_N and is given by a linear combination of weight-3 planar f -graphs that can be recast as bipartite graphs, which manifest important properties of ABJM amplitudes. We provide evidence that it contains sufficient information to reconstruct individual amplitudes, despite the absence of squared amplitudes at odd loops. The extraction of the four-point amplitude is already non-trivial and closely parallels the extraction of five-point amplitudes in $\mathcal{N} = 4$ super Yang-Mills (SYM) from weight-4 f -graphs: we comment on this similarity and provide new results for $n = 4$ ABJM loop integrand up to $L = 6$. For higher multiplicities, based on Yangian invariants (including BCFW building blocks for tree amplitudes) and an appropriate basis of planar dual conformal invariant(DCI) integrands, we disentangle six-point integrands up to two loops and eight-point tree amplitude from the squared amplitudes. Our results suggest that ABJM amplitudes of arbitrary multiplicity and loop order can be reconstructed from squared amplitudes, closely paralleling the role of f -graphs in $\mathcal{N} = 4$ SYM.

Contents

1	Introduction	1
2	Four-point ABJM amplitudes from f-graphs	5
2.1	How to disentangle products of lower loops from planar f -graphs?	5
2.2	From bipartite f -graphs to log of amplitudes and negative geometries	8
3	Six-point ABJM amplitudes from f-graphs	10
3.1	Squaring tree amplitudes and leading singularities	10
3.2	Extracting one and two-loop integrands	12
4	Eight-point ABJM amplitudes from f-graphs	14
5	Discussions and Outlook	16
A	The definition of three-loop planar DCI integrands	17
B	Proof of Theorem (4.3)	18

1 Introduction

Recent years have witnessed remarkable progress in understanding scattering amplitudes in Quantum Field Theory, particularly in superconformal theories like four-dimensional $\mathcal{N} = 4$ super-Yang-Mills (SYM) and three-dimensional $\mathcal{N} = 6$ Chern-Simons-matter theory known as Aharony-Bergman-Jafferis-Maldacena (ABJM) [1, 2]. In both theories, new mathematical structures in the planar integrands of all-loop amplitudes have been discovered, which share important hidden symmetry such as the Yangian symmetry [3–8], deep connections to the positive Grassmannian [9–12] and the remarkable geometry known as the amplituhedra [13–19]. A long-standing open question is whether the amplitude/Wilson loop/correlator triality, analogous to the well-established SYM case [20–24], also exists in ABJM theory (*c.f.* [25–31]). A significant step in this direction was the recent discovery of a hidden permutation symmetry that unifies amplitudes with different multiplicities and loop orders under the constraint $N=n+L$ [32], offering a powerful new framework for studying the squared amplitudes, or cross-section, as well as (loop integrands of) scattering amplitudes themselves in ABJM theory.

In SYM theory, inspired by correlator/amplitude duality, the squared amplitude can be packaged into a permutation-invariant object F_N , represented as a sum over planar f -graphs. Each f -graph is a rational function of dual coordinates and enjoys an S_N permutation symmetry acting on both external and internal dual points. Remarkably, by taking n -gon lightlike limits, F_N simultaneously encodes all n -point L -loop amplitudes

with $n + L = N$. In this framework, individual loop integrands can be efficiently extracted from f -graphs. At $n = 4$, the L -loop integrand is obtained by identifying all four-faces of $(4 + L)$ -vertex f -graphs, allowing the integrand to be determined in principle up to $L = 12$ [33–35]. At five-point, the L -loop parity-even integrand can be extracted from five-faces of $(5 + L)$ -vertex f -graphs, while the parity-odd contribution of L -loop can be obtained from penta-wheel subtopologies of $(6 + L)$ -vertex f -graphs [36]. At higher multiplicity, although a simple graphical prescription is no longer available, it is conjectured that all-loop integrands can still be obtained from f -graphs by constructing suitable integrand ansatz [37]. As a result, the planar f -graph representation has become a powerful tool for organizing and computing loop integrands in SYM.

In contrast, loop integrands in three-dimensional ABJM theory are much less explored. Using generalized unitarity [38] and positive geometry, planar integrands up to eight points at two-loop level were constructed [19, 39–42], as well as the four-point integrand up to five loops in a bipartite representation based on the ABJM amplituhedron [18]. Meanwhile, although a fully permutation-invariant squared amplitude was also defined, several new challenges arise when attempting to extract individual amplitudes from this squared object. First, ABJM squared amplitudes exist only for even multiplicity and even loop-level, making it a priori difficult to extract the odd-loop integrand. Second, the available f -graph data are currently limited to ten points, where certain free parameters still remain due to Gram determinant identities in three dimensions.

The central question addressed in this paper is whether the three-dimensional object F_N nevertheless contains complete information about individual amplitudes, or equivalently, whether one can systematically extract all scattering amplitudes directly from the squared amplitude. We show that, based on the collection of Yangian invariants and an appropriate basis of planar dual conformal integrands, it is indeed possible to disentangle the contributions of individual amplitudes from the permutation-invariant combination. Our results provide strong evidence that scattering amplitudes of arbitrary multiplicity and loop order can be extracted from three-dimensional f -graphs. Before moving on to our main results, let us first review the generating function for squared amplitudes in ABJM theory.

Squared amplitudes in ABJM In chiral superspace [43], the n -point superamplitude \mathcal{A}_n of ABJM theory satisfies super-momentum conservation:

$$\mathcal{A}_n(\lambda, \eta) = \delta^3(P)\delta^6(Q)\mathcal{A}_n(\lambda, \eta), \quad (1.1)$$

$$P^{\alpha\dot{\alpha}} = \sum_{i=1}^n (-1)^i \lambda_i^\alpha \lambda_i^{\dot{\alpha}}, \quad Q^{\alpha A} = \sum_{i=1}^n (-1)^i \lambda_i^\alpha \eta_i^A. \quad (1.2)$$

The Grassmann variables η_i^A ($A = 1, 2, 3$) encode the external states. In ABJM theory, the only non-vanishing amplitudes are those with an even number of particles, $n = 2k$, and in the middle sector $A_{n=2k} \sim \eta^{3k}$. Perturbatively,

$$A_n = \sum_{L=0}^{\infty} a^L \int d^{3L}x A_n^{(L)}(x_1, x_2, \dots, x_n, x_{n+1}, \dots, x_{n+L}), \quad (1.3)$$

where a denotes the coupling constant; the external dual points are defined through $p_i = x_{i+1} - x_i \equiv x_{i,i+1}$ for $i = 1, \dots, n$ which form a light-like n -gon, and in addition there are L generic loop/internal points for $i = n+1, \dots, n+L$; by definition, $A_n^{(L)}$ is permutation symmetric among these internal points $x_{n+1}, x_{n+2}, \dots, x_{n+L}$.

The (integrand of the) squared ABJM amplitude was recently introduced in [32] in a manner analogous to the SYM case [37, 44–46]. It is defined as the sum over the squares of all component amplitudes, namely

$$M_n^{(L)} := \frac{1}{2} \sum_{\ell=0}^L \overline{A_n^{(\ell)}}(\lambda, \partial_\eta) A_n^{(L-\ell)}(\lambda, \eta) \Big|_{\eta=0}, \quad (1.4)$$

where the conjugated amplitude $\overline{A_n^{(\ell)}}$ means

$$\overline{A_n^{(\ell)}}(\lambda, \partial_\eta) = (-1)^\ell A_n^{(\ell)}(\lambda, \eta) \Big|_{\eta \rightarrow \partial_\eta}, \quad (1.5)$$

Notice that the integrand picks up an additional $(-1)^\ell$ factor due to the charge conjugation. More importantly, this sign forces all odd-loop squared amplitudes to vanish, which plays a crucial role in the unification of loops and legs after squaring. More explicitly at the loop-level,

$$A_n^{(\ell)} A_n^{(L-\ell)} = \sum_{\sigma \in S_L} A_n^{(\ell)}(x_{\sigma(1)}, \dots, x_{\sigma(\ell)}) \times A_n^{(L-\ell)}(x_{\sigma(\ell+1)}, \dots, x_{\sigma(L)}) \quad (1.6)$$

For example, with the normalization $A_4^{(0)} = \frac{1}{\langle 12 \rangle \langle 23 \rangle}$, the four-point squared amplitudes are

$$M_4^{(0)} = \frac{1}{2} \frac{1}{x_{13}^2 x_{24}^2}, M_4^{(2)} = A_4^{(0)} A_4^{(2)} - \frac{1}{2} [A_4^{(1)}]^2, M_4^{(4)} = A_4^{(0)} A_4^{(4)} - A_4^{(1)} A_4^{(3)} + \frac{1}{2} [A_4^{(2)}]^2. \quad (1.7)$$

A remarkable feature of the squared amplitudes/cross-sections is a hidden S_{n+L} permutation symmetry which unifies these objects with different n and L . As discovered in [32], there exists a single object $F_N(x_1, \dots, x_N)$ which is symmetric in all $N := n+L$ points, that packages squared amplitudes, $M_n^{(L)}$, with different n, L (unifying “loops and legs”); the latter are obtained by taking n -gon lightlike limits similar to SYM case [33]:

$$\lim_{x_{12}^2, \dots, x_{n1}^2 \rightarrow 0} \sigma_n F_N \equiv \text{Res}_{n\text{-gon}} F_N = M_n^{(L)}(x_1, \dots, x_N), \quad (1.8)$$

where $\sigma_n := x_{12}^2 x_{23}^2 \dots x_{n1}^2$, and taking the n -gon lightlike residue, $x_{i,i+1}^2 = 0$ for $i = 1, \dots, n$, is denoted as $\text{Res}_{n\text{-gon}}$. The remarkable property that F_N is invariant under S_N permutation of x_1, \dots, x_N means that it admits a representation in terms of f -graphs (with weight-3 for ABJM, as opposed to those weight-4 ones in SYM) [32, 47]. In ABJM theory, to manifest the vanishing of odd-particle amplitudes, its f -graphs cannot contain odd cycles and therefore must be bipartite. On the other hand, dual conformal invariance in $D = 3$ requires the integrand to have conformal weight 3 at each point, which implies that the valency of each vertex in the f -graph is 3. Combining these two constraints, the

f -graphs are thus weight-3 *bipartite graphs*.¹ where each solid line $i-j$ denotes the pole x_{ij}^2 in the denominator and dashed line $i-j$ denotes an x_{ij}^2 factor in the numerator; the S_N permutation invariance indicates that we must sum over all possible labeling to obtain the rational function associated with any f -graph. For example, at $N = 6$, the only possible bipartite graph is the following $K_{3,3}$ graph and

$$\begin{aligned}
F_6 &= 2 \times \langle \text{K}_{3,3} \rangle = 2 \times \left(\frac{1}{72} \frac{1}{x_{12}^2 x_{23}^2 x_{34}^2 x_{45}^2 x_{56}^2 x_{61}^2 x_{14}^2 x_{25}^2 x_{36}^2} + S_6 \text{ perms} \right) \\
&= \frac{2}{x_{12}^2 x_{23}^2 x_{34}^2 x_{41}^2 x_{13}^2 x_{24}^2} \left(\frac{x_{12}^2 x_{34}^2}{x_{16}^2 x_{26}^2 x_{35}^2 x_{45}^2 x_{56}^2} + \frac{x_{13}^2 x_{24}^2}{x_{16}^2 x_{36}^2 x_{25}^2 x_{45}^2 x_{56}^2} + \frac{x_{14}^2 x_{23}^2}{x_{16}^2 x_{46}^2 x_{25}^2 x_{35}^2 x_{56}^2} + 5 \leftrightarrow 6 \right) \\
&+ \frac{2}{x_{12}^2 x_{23}^2 x_{34}^2 x_{41}^2 x_{13}^2 x_{24}^2} \left(\frac{x_{12}^2 x_{23}^2 x_{31}^2}{x_{16}^2 x_{26}^2 x_{36}^2 x_{15}^2 x_{25}^2 x_{35}^2} + 3 \text{ cyc} \right),
\end{aligned} \tag{1.9}$$

where the second line is the three-dimensional double triangle integral, which evaluates to elliptic polylogarithm functions as computed in [48], and the last line is nothing but squared triangles. After taking the lightlike limit, it gives the four-point two-loop and six-point tree-level squared amplitudes, respectively:

$$\begin{aligned}
\text{Res}_{4\text{-gon}} 2 \times \langle \text{K}_{3,3} \rangle &= \frac{2}{x_{15}^2 x_{35}^2 x_{56}^2 x_{26}^2 x_{46}^2} + (5 \leftrightarrow 6) = M_4^{(2)} \\
\text{Res}_{6\text{-gon}} 2 \times \langle \text{K}_{3,3} \rangle &= \frac{2}{x_{14}^2 x_{25}^2 x_{36}^2} = M_6^{(0)}
\end{aligned} \tag{1.10}$$

Meanwhile, due to the Gram identities $\det_{1 \leq i, j \leq 6} x_{ij}^2 = 0$ in $D = 3$, we can also write these bipartite f -graphs in terms of planar ones, for example

$$2 \langle \text{K}_{3,3} \rangle = \langle \text{planar}_1 \rangle - \langle \text{planar}_2 \rangle + \frac{1}{2} \langle \text{planar}_3 \rangle, \tag{1.11}$$

Although the vanishing of odd-particle amplitude/cut is not manifest by this planar representation, it is useful to extract four-point lower loop integrands as we show later.

This paper is organized as follows. In section 2, we first explain the challenges in extracting amplitude from the squared object. Then we show how to adapt the method in [36] to extract four-point $(L-1)$ -loop integrand from planar f -graph representation of F_{4+L} . We also comment on the relationship between squaring and taking the logarithm at four-point. In section 3, we move on to the six-point extraction. After introducing a more compact formula for the squared tree amplitude, we demonstrate that the six-point amplitude up to $L = 2$ can be obtained from f -graphs by writing down a suitable

¹ The lowest-point $F_4 = \frac{1}{2} \langle \triangle \rangle$ is an exception by being planar but not bipartite. This is similar to SYM where $F_{N \geq 6}^{\text{SYM}}$ are planar but F_5^{SYM} is nonplanar.

DCI integrand ansatz that satisfies cyclicity, reflection symmetry, and a soft-cut condition relating higher- and lower-loop orders. In section 4, we show that the same method can be applied to the eight-point amplitude at tree-level.

2 Four-point ABJM amplitudes from f -graphs

In this section, we discuss how to extract L -loop integrand of four-point amplitudes from f -graphs with $4+L$ points. In $D = 3$, each dual point x_i can be embedded into a five-dimensional space as $X_i = (\frac{1}{2}x_i^2, 1, x_i^\mu)$. The four-point integrand in ABJM theory is slightly more intricate than in SYM: in addition to its dependence on x_{ij}^2 , it contains a parity-odd structure naturally defined in the embedding space, which is constructed from the contraction of the five-dimensional epsilon tensor with five X_i 's. At four-point the ϵ tensor is introduced as

$$\epsilon_\ell \equiv \epsilon(\ell, 1, 2, 3, 4) = 2\epsilon_{abcde} X_1^a X_2^b X_3^c X_4^d X_\ell^e, \quad (2.1)$$

where $\ell = 5, 6, \dots, 4+L$, and ϵ_ℓ is normalized such that

$$\epsilon_\ell^2 = -x_{13}^2 x_{24}^2 (x_{24}^2 x_{\ell 1}^2 x_{\ell 3}^2 + x_{13}^2 x_{\ell 2}^2 x_{\ell 4}^2). \quad (2.2)$$

More generally,

$$\epsilon(a_1, a_2, a_3, a_4, *)\epsilon(b_1, b_2, b_3, b_4, *) = -\frac{1}{2} \det[(a_i \cdot b_j)]. \quad (2.3)$$

Recall that, for odd/even L , the L -loop integrand is parity odd/even, which then must contain odd/even powers of such ϵ tensors. For example, the one-loop integrand is the box integral with an ϵ numerator [49]

$$A_4^{(1)} = A_4^{(0)} \frac{\epsilon_\ell}{x_{\ell 1}^2 x_{\ell 2}^2 x_{\ell 3}^2 x_{\ell 4}^2} \quad (2.4)$$

At two-loop, the integrand can be written as a linear combination of the double box (with two such ϵ tensors contracted in the numerator) and the double triangle [49]

$$A_4^{(2)} = \frac{\epsilon_5 \epsilon_6}{x_{15}^2 x_{16}^2 x_{25}^2 x_{35}^2 x_{36}^2 x_{46}^2} - \frac{x_{13}^4}{x_{15}^2 x_{16}^2 x_{35}^2 x_{36}^2 x_{56}^2} + (5 \leftrightarrow 6) + (13 \leftrightarrow 24) \quad (2.5)$$

2.1 How to disentangle products of lower loops from planar f -graphs?

Recall that in SYM theory, extracting the amplitude $A_4^{(L)}$ from F_{4+L} is purely graphical: one simply identifies all 4-faces of planar f -graphs and then takes the lightlike limit [33, 50]. Moreover, the product of lower loop amplitude $A_4^{(\ell)} A_4^{(L-\ell)}$ correspond to 4-cycles that divide the planar f -graph into “interior” and “exterior”, containing ℓ and $L - \ell$ vertices, respectively.

Comparing with (2.5), the first subtlety in ABJM theory is that F_6 is manifestly parity-even and contains no ϵ -tensor. In fact, using (2.3), one finds

$$-2\epsilon_i \epsilon_j = x_{13}^2 x_{24}^2 x_{ij}^2 - N^c[i|j], \quad (2.6)$$

where $N^c[i|j] = x_{24}^2 x_{i1}^2 x_{j3}^2 + \text{cyc}(1234)$. Substituting this into (2.5) yields

$$A_4^{(2)} = -\frac{x_{2,4}^2 x_{1,3}^4}{2x_{1,5}^2 x_{1,6}^2 x_{2,5}^2 x_{3,5}^2 x_{3,6}^2 x_{4,6}^2} + \frac{x_{2,4}^2 x_{1,3}^2}{2x_{1,6}^2 x_{2,5}^2 x_{3,5}^2 x_{4,6}^2 x_{5,6}^2} + \frac{x_{2,6}^2 x_{4,5}^2 x_{1,3}^4}{2x_{1,5}^2 x_{1,6}^2 x_{2,5}^2 x_{3,5}^2 x_{3,6}^2 x_{4,6}^2 x_{5,6}^2} \quad (2.7)$$

$$+ \frac{x_{2,4}^2 x_{1,3}^2}{2x_{1,5}^2 x_{2,5}^2 x_{3,6}^2 x_{4,6}^2 x_{5,6}^2} - \frac{x_{1,3}^4}{2x_{1,5}^2 x_{1,6}^2 x_{3,5}^2 x_{3,6}^2 x_{5,6}^2} + (5 \leftrightarrow 6) + (13 \leftrightarrow 24).$$

This form only depends on $x_{i,j}^2$, though at the cost of introducing additional topologies such as the kissing-triangle (colored red in (2.7)), which notably lacks the mutual pole x_{56}^2 in the denominator. The appearance of such kissing topologies is the first indication that one cannot obtain the 4-point L -loop integrand simply by locating 4-faces of planar $(4+L)$ -vertex f -graphs. The topology of the graph alone does not reveal whether a given contribution corresponds to an L -loop integrand or to a product of lower-loop amplitudes. A similar obstruction was observed in extracting higher-multiplicity amplitudes in SYM theory [37].

On the other hand, extracting products of lower-loop integrands cannot proceed as in four dimensions. For instance, consider the six-point planar f -graphs

$$F_6 = \text{[Diagram 1]} - \text{[Diagram 2]} + \frac{1}{2} \text{[Diagram 3]}, \quad (2.8)$$

where the red lines denote a 4-cycle that separates the planar graph into an ‘interior’ and an ‘exterior’, each containing exactly one vertex. By analogy with the SYM case, one might expect that this would correspond to $[A_4^{(1)}]^2$. However, it actually gives

$$-\frac{x_{13}^2 x_{24}}{x_{15}^2 x_{16}^2 x_{26}^2 x_{35}^2 x_{36}^2 x_{45}^2} + (5 \leftrightarrow 6) + (13 \leftrightarrow 24) + \frac{1}{2} \frac{x_{13}^4 x_{24}^2 x_{56}^2}{x_{15}^2 x_{16}^2 x_{25}^2 x_{26}^2 x_{35}^2 x_{36}^2 x_{45}^2 x_{46}^2} \quad (2.9)$$

$$= -2 \frac{\epsilon_1 \epsilon_2}{x_{15}^2 x_{25}^2 x_{35}^2 x_{45}^2 x_{16}^2 x_{26}^2 x_{36}^2 x_{46}^2} - \frac{1}{2} \frac{x_{13}^4 x_{24}^2 x_{56}^2}{x_{15}^2 x_{16}^2 x_{25}^2 x_{26}^2 x_{35}^2 x_{36}^2 x_{45}^2 x_{46}^2} \neq [A_4^{(1)}]^2.$$

where in the second line we used the identity (2.6).

It turns out that we can extract the $(L-1)$ -loop integrand, which is an odd-loop integrand for L even, from the planar $(4+L)$ -point f -graphs in close analogy with the five-point parity-odd part in the SYM case. As we have checked to $L = 6$ at least, one can assume that odd-loop integrands always take the form written as

$$A_4^{(L-1)} = \epsilon_\ell \hat{A}_4^{(L-1)}, \quad (2.10)$$

and there will never be an epsilon tensor involving two or more internal points. To isolate one-loop contribution (2.4) from $-A_4^{(1)} A_4^{(L-1)}$ in (1.4), by using (2.6), we obtain

$$-A_4^{(1)} A_4^{(L-1)} = -\frac{\epsilon_L}{x_{L1}^2 x_{L2}^2 x_{L3}^2 x_{L4}^2} \epsilon_L \hat{A}_4^{(L-1)} = \frac{1}{2} \frac{x_{13}^2 x_{24}^2 x_{iL}^2 + \dots}{x_{L1}^2 x_{L2}^2 x_{L3}^2 x_{L4}^2} \hat{A}_4^{(L-1)}. \quad (2.11)$$

Therefore, to isolate the contribution of the odd-loop integrand, it is sufficient to identify all **box-wheel** subgraphs, namely planar four-cycles that enclose one internal vertex, with four propagators (spokes) connecting this vertex to the four corners of the box (see Fig. 1). Each such box-wheel necessarily has a numerator line from its central vertex to some other vertex in the remainder of the f -graph. Removing the box-wheel and marking the endpoint of that numerator produces a new graph that contributes directly to the $(L - 1)$ -loop integrand which is purely parity-odd, with its coefficient doubled and the marked vertex ℓ carrying numerator ϵ_ℓ :

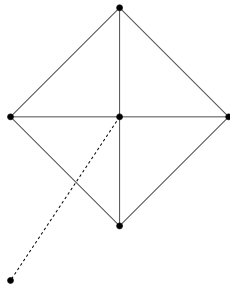


Figure 1: boxwheel

As an example, in (2.8) only the last 6-point f -graph contains the box-wheel subgraph,

(2.12)

which corresponds precisely to $A_4^{(1)} \times A_4^{(1)}$. Similarly, at three loops there are 11 planar f -graphs with non-vanishing coefficients containing the box-wheel subgraph. We obtained 13 planar integrand seeds, including one kissing topology, eight ladder-type topologies, and 4 tennis-court topologies (listed in the Appendix A). We also checked that they reproduce the result in [18, 51]. At five loops, this procedure leads to a new planar representation of the integrand (recorded in an ancillary Mathematica file), in contrast to the bipartite and non-planar representation obtained in [18]. Although expressed in different forms, the two representations can be explicitly checked to be equivalent.

Finally, before moving to the next subsection—where we focus on the logarithm of the amplitude, we emphasize that we can already recursively obtain the L -loop planar integrand from $(4 + L)$ -point f -graphs. Assuming that all lower-loop integrands are known from f -graphs with $N \leq 4 + L$ points, then from $(4 + L + 2)$ -point f -graphs, once the $(L + 1)$ -loop integrand is identified, one can subtract all lower-loop products from $M_4^{(L+2)}$ to obtain the $(L + 2)$ -loop amplitude with all the products of ϵ_i in odd-loop, which can be further simplified using (2.6). We note that after doing so systematically, one obtains an even nicer representation of the planar loop integrand, which we leave to future work.

2.2 From bipartite f -graphs to log of amplitudes and negative geometries

In this subsection, we start from the bipartite f -graph representation of the squared amplitude in ABJM theory and connect it to the logarithm of the 4-point amplitude:

$$\log R_4 = \sum_{L=0}^{\infty} a^L (\log R_4)^{(L)}, \quad (2.13)$$

where $R_4 \equiv \frac{A_4}{A_4^{(0)}}$. Starting from a rewriting of the squared amplitudes

$$M_4 = \frac{1}{2} (A_4^{(0)})^2 \exp \left[\log \frac{A_4(-a)A_4(a)}{[A_4^{(0)}]^2} \right] = M_4^{(0)} \exp [\log R_4(a) + \log R_4(-a)], \quad (2.14)$$

we can express $M_4^{(L)}$ in terms of $(\log R_4)^{(\ell)}$ with even ℓ only. For example,

$$\begin{aligned} \frac{M_4^{(0)}}{(A_4^{(0)})^2} &= \frac{1}{2}, \quad \frac{M_4^{(2)}}{(A_4^{(0)})^2} = (\log R_4)^{(2)}, \quad \frac{M_4^{(4)}}{(A_4^{(0)})^2} = (\log R_4)^{(4)} + [(\log R_4)^{(2)}]^2, \\ \frac{M_4^{(6)}}{(A_4^{(0)})^2} &= (\log R_4)^{(6)} + 2(\log R_4)^{(4)}(\log R_4)^{(2)} + \frac{2}{3} [(\log R_4)^{(2)}]^3. \end{aligned} \quad (2.15)$$

An important feature of $(\log R_4)^{(\ell)}$ with $\ell > 1$ is its ‘‘bipartite pole structures’’, as studied in [18] using negative geometries. For example, at two loops

$$\begin{aligned} (\log R_4)^{(2)} &= \frac{M_4^{(2)}}{(A_4^{(0)})^2} = \lim_{x_{i,i+1}^2 \rightarrow 0} \xi_4 x_{13}^2 x_{24}^2 \times 2 \cdot \begin{array}{c} \bullet \\ \circ \\ \bullet \\ \circ \end{array} \begin{array}{c} \bullet \\ \circ \\ \bullet \\ \circ \end{array} \\ &= \begin{array}{c} \bullet \\ \circ \\ \bullet \\ \circ \end{array} \begin{array}{c} \bullet \\ \circ \\ \bullet \\ \circ \end{array} = \frac{2x_{13}^2 x_{24}^2}{x_{51}^2 x_{53}^2 x_{62}^2 x_{64}^2 x_{56}^2} \quad (5 \leftrightarrow 6), \end{aligned} \quad (2.16)$$

where each black node i represents the pole $s_i := x_{i1}^2 x_{i3}^2$, while each white node j represents $t_j = x_{j2}^2 x_{j4}^2$; the link between two internal dual points denotes the pole x_{ij}^2 . For higher loops, there will be more than one bipartite topologies, and these bipartite graphs from negative geometries fully determine the pole structures of $\log R_4$.

Using (2.15), we can obtain the log of amplitudes recursively at even loops from the squared amplitudes. Inspired by [18], we can regroup the full results into connected bipartite topologies. To achieve this, we can write down an ansatz for each bipartite topology which has the correct DCI weight and symmetry properties using ϵ_i and x_{ij}^2 (not including the mutual ones). For example, at four loops, there are 3 bipartite topologies, *i.e.* chain, star and box topology.

$$(\log R_4)^{(4)} = -C - S + B, \quad (2.17)$$

where

interesting to fix the Gram by other graphical rules at $L = 6$ to see whether the largest coefficient is also 2^5 given by $K_{3,11}$.

3 Six-point ABJM amplitudes from f -graphs

3.1 Squaring tree amplitudes and leading singularities

In ABJM theory, the $(n = 2k)$ -point tree-level amplitude is associated with $(n - 3)$ -dimensional cells of the orthogonal Grassmannian $OG_+(k, 2k)$. More precisely, the BCFW building blocks appearing in the tree-level recursion can be written as residues of the integral [10, 12]

$$\mathcal{A}_{n=2k} = \int \frac{d^{k \times 2k} C}{GL(k)} \frac{\delta^{\frac{k(k+1)}{2}}(C \cdot C^T)}{\prod_{i=1}^k M_i} \delta^{2k|3k}(C \cdot \Lambda) \quad (3.1)$$

where the dot products are defined according to the n -dimensional splitting signature metric $\eta = \text{diag}(1, -1, \dots, +1, -1, +1)$, the kinematic data including the Grassmann variables is encoded in $\Lambda_i = (\lambda_i, \eta_i)$, and the minors are defined as $M_i = (i, i+1, \dots, i+k-1)$. Localizing $M_i = 0$ restricts it to an $(n - 3)$ -dimensional subspace by evaluating the residues on the loci of $M_i = 0$, corresponding to cells with co-dimension $\frac{(k-2)(k-3)}{2}$ of the positive orthogonal Grassmannian $OG_+(k, 2k)$. For example, at $n = 4, 6$ the tree amplitude is given by the top cell, while for $n = 8$ the BCFW terms are given by co-dimension one cells corresponding to $M_i = 0$ for $i = 1, 2, 3, 4$. Also note that since the orthogonal constraint is quadratic in C , $2 \times 2^{k-2}$ solutions are split into positive and negative branches, which satisfy $\frac{M_I}{M_{\bar{I}}} = \pm 1$.

From (super)momentum conservation, the orthogonal Grassmannian matrix C can be fixed to be

$$C = \begin{pmatrix} \lambda \\ \hat{C} \end{pmatrix}, \quad (3.2)$$

then we write the full amplitudes as sum over cells σ , the branches \pm and solutions:

$$\begin{aligned} \mathcal{A}_n &= A_n \delta^3(P) \delta^6(Q) \equiv \sum_{\sigma} \sum_{\pm} \sum_{\text{sol}} f_{\sigma, \pm, \text{sol}} \delta^{k-2}(\hat{C}_{\sigma, \pm, \text{sol}} \cdot \eta) \delta^3(P) \delta^6(Q) \\ &\equiv \delta^3(P) \delta^6(Q) \sum_{\sigma} \sum_{\pm} \sum_{\text{sol}} \text{LS}_{\pm, \text{sol}}[\sigma_i] \end{aligned}$$

When computing the product of two super-functions according to (1.4), we have

$$\begin{aligned} f \delta^{k-2}(\hat{C} \cdot \eta) \star f' \delta^{k-2}(\hat{C}' \cdot \eta) &= f f' \prod_{I=1}^3 \prod_{j=1}^{k-2} \sum_{\alpha=1}^n i^{\text{odd}(\alpha)} \hat{C}'_{j, \alpha} \partial_{\eta_{\alpha, I}} \prod_{I'=1}^3 \prod_{j'=1}^{k-2} \sum_{\alpha'=1}^n i^{\text{odd}(\alpha')} \hat{C}_{j, \alpha} \eta_{\alpha', I'} \\ &= f f' \prod_{I=1}^3 \sum_{\alpha \in S_{k-2}} \text{sgn}(\sigma) \prod_{j=1}^{k-2} \sum_{\alpha=1}^n (-1)^\alpha \hat{C}_{j, \alpha} \hat{C}'_{\sigma(j), \alpha} \\ &= f f' \det(\hat{C} \cdot \hat{C}'^T)^3, \end{aligned} \quad (3.3)$$

where in the second line we used $\partial_{\eta_{\alpha,I}}\eta_{\alpha',I'} = \delta_{\alpha,\alpha'}\delta_{I,I'}$ and the anti-commutativity property of Grassmannian variables. An immediate consequence is that the square of any superfunction itself vanishes due to the orthogonal condition $\hat{C} \cdot \hat{C}^T = 0$.

At six points, only the top cell contributes which can be parametrized as

$$C_{\pm} = \begin{pmatrix} \lambda_1 & \lambda_2 & \lambda_3 & \lambda_4 & \lambda_5 & \lambda_6 \\ \langle 35 \rangle & \langle 24 \rangle & \langle 51 \rangle & \langle 62 \rangle & \langle 13 \rangle & \langle 46 \rangle \end{pmatrix}, \quad C_{-} = \begin{pmatrix} \lambda_1 & \lambda_2 & \lambda_3 & \lambda_4 & \lambda_5 & \lambda_6 \\ \langle 35 \rangle & -\langle 24 \rangle & \langle 51 \rangle & -\langle 62 \rangle & \langle 13 \rangle & -\langle 46 \rangle \end{pmatrix}, \quad (3.4)$$

where \pm corresponds to the positive/negative branch, and they give two leading singularities

$$\text{LS}_{\pm} = \frac{\delta^3(C_{\pm} \cdot \eta)}{2c_1^{\pm}c_2^{\pm}c_3^{\pm}}, \quad (3.5)$$

where

$$\begin{aligned} c_1^{\pm} &= -\langle 5|135|2 \rangle \mp \langle 13 \rangle \langle 46 \rangle \\ c_2^{\pm} &= \pm \langle 6|246|3 \rangle \mp \langle 24 \rangle \langle 51 \rangle \\ c_3^{\pm} &= -\langle 1|135|4 \rangle \mp \langle 35 \rangle \langle 62 \rangle \end{aligned} \quad (3.6)$$

After stripping of the $\delta^3(P)\delta^6(Q)$, the tree amplitude A_6 is proportional the sum of two branches

$$A_6 = \alpha(\text{LS}_+ + \text{LS}_-) \quad (3.7)$$

The six-point case provides a trivial example of extracting tree amplitude similar to [37], where we only need to fix the overall coefficient α by comparing it to $M_6^{(0)}$ (1.10). Using (3.3), the square of LS_{\pm}^2 vanishes, and only the product between positive and negative branches contributes to the squared amplitudes

$$M_6^{(0)} = \frac{1}{2}A_6^2 = \alpha^2\text{LS}_+\text{LS}_- = \frac{\alpha^2 \det(C_+ \cdot C_-)^3}{4(c_1^+c_1^-)(c_2^+c_2^-)(c_3^+c_3^-)}. \quad (3.8)$$

The determinant in the numerator becomes

$$-\langle 13 \rangle^2 - \langle 35 \rangle^2 - \langle 51 \rangle^2 - \langle 24 \rangle^2 - \langle 46 \rangle^2 - \langle 62 \rangle^2 = -s_{135} \quad (3.9)$$

while the factors in the denominators can be simplified to be

$$c_1^+c_1^- = x_{14}^2s_{135}, c_2^+c_2^- = -x_{25}^2s_{135}, c_3^+c_3^- = x_{36}^2s_{135}. \quad (3.10)$$

Therefore the square of ansatz (3.7) becomes

$$M_6^{(0)} = \frac{2\alpha^2}{x_{14}^2x_{25}^2x_{36}^2}. \quad (3.11)$$

Comparing to (1.10), we can obtain $\alpha = \pm 1$, which gives the correct result [52] by choosing the positive sign. The correlator can never predict this sign since the duality (1.8) only gives the square of the amplitude. If we had chosen the wrong sign here, it would affect higher-loop amplitudes.

For higher loops, it is convenient to introduce the shifted tree amplitude $A_6^s(\bar{1}\bar{2}\bar{3}\bar{4}\bar{5}\bar{6}) = A_6(\bar{2}\bar{3}\bar{4}\bar{5}\bar{6}\bar{1}) = -i(\text{LS}_+ - \text{LS}_-)$, whose square also gives $M_6^{(0)}$. Meanwhile the mixed product $A_6 \star A_6^s = 0$. This vanishing result is natural: the product must yield a parity-even object, whereas A_6 and A_6^s have opposite parity.

3.2 Extracting one and two-loop integrands

Following the strategy of [37], we attempt to extract the six-point loop integrand from the f -graph data by introducing the ansatz

$$A_6^{(L)} = A_6 I^{(L)} + A_6^s I_s^{(L)}. \quad (3.12)$$

In addition to having the correct dual conformal weight, the ansatz must obey several physical constraints such as cyclicity, reflection and parity[28, 42]

$$\begin{aligned} A_n(\bar{1}2\bar{3} \dots n) &= (-1)^{\frac{n}{2}-1} A_n(\bar{3}4\bar{5} \dots 2) \\ A_n(\bar{1}2\bar{3} \dots n) &= (-1)^{\frac{n(n-2)}{8}+L} A_n(\bar{1}n \dots 4\bar{3}2), \\ A_n(\dots, -\Lambda_i, \dots) &= (-1)^{F_i} A_n(\dots, \Lambda_i, \dots) \end{aligned} \quad (3.13)$$

where F_i denotes fermion number of leg i . These relations implies $I^{(L)}$ and $I_s^{(L)}$ are invariant under cyclic by 2 and pick up an $(-1)^L$ under reflection. Also $I^{(L)}$ should be parity even (odd) at even (odd) loop, while $I_s^{(L)}$ has the opposite parity.

Let us show that, at $L = 2$, comparing the squared integrand ansatz with the result obtained from the f -graph completely fixes the one-loop integrand as well as the parity-even part of the two-loop integrand. More generally, when squaring the ansatz (3.12) at L loops, the even-loop squared amplitude $M_6^{(L)}$ contains contribution from $I^{(L)}, I^{(L-1)}, I_s^{(L)}$ as follows

$$A_6 I^{(L)} * A_6 I^{(0)} + A_6 I^{(L-1)} * A_6 I^{(1)} + A_6^s I_s^{(L-1)} * A_6^s I_s^{(1)} \quad (3.14)$$

which gives some ambiguity $I_{\text{parity odd}}$ and $I_{\text{parity even}}$ that is invisible in f -graph

$$\begin{aligned} I^{(L-1)} &\rightarrow I^{(L-1)} + I_{\text{parity odd}}, I_s^{(L-1)} \rightarrow I_s^{(L-1)} + I_{\text{parity even}} \\ I^{(L)} &\rightarrow I^{(L)} - I_{\text{parity odd}} I^{(1)} - I_{\text{parity even}} I_s^{(1)}, \end{aligned} \quad (3.15)$$

where $I_{\text{parity odd}}$ and $I_{\text{parity even}}$ are any combination $(L-1)$ -loop integrands which are parity odd/even. In fact, (3.15) is the only form of ambiguity arising from the duality at the loop level.

More explicitly, at two loops (1.4) becomes

$$\frac{M_6^{(2)}}{M_6^{(0)}} = I^{(2)} - \frac{1}{2}(I_s^{(1)})^2 - \frac{1}{2}(I^{(1)})^2 \quad (3.16)$$

Then we write down a linear independent basis of loop integrands. At one loop, we only have parity-even triangles (with $(i, j, k) = (1, 3, 5)$ or $(2, 4, 6)$), and parity-odd boxes with ϵ numerator ($1 \leq i < j < k < m \leq 6$)

$$\begin{aligned} \text{tri}[i, j, k] &= \frac{\sqrt{x_{ij}^2 x_{jk}^2 x_{ki}^2}}{x_{\ell i}^2 x_{\ell j}^2 x_{\ell k}^2} \equiv \frac{(i \cdot j \cdot k)}{x_{\ell i}^2 x_{\ell j}^2 x_{\ell k}^2} \quad \text{parity-even triangle} \\ \text{box}[i, j, k, m] &= \frac{\epsilon(\ell, i, j, k, m)}{x_{\ell i}^2 x_{\ell j}^2 x_{\ell k}^2 x_{\ell m}^2} \quad \text{parity-odd box} \end{aligned} \quad (3.17)$$

Among the 15 boxes, five linear relations follow from the 5-term Schouten identity of the 5D Levi-Civita tensor,

$$\text{box}[i, j, k, l] - \text{box}[j, k, l, p] + \text{box}[k, l, p, i] - \text{box}[l, p, i, j] + \text{box}[p, i, j, k] = 0, \quad (3.18)$$

leaving an ansatz with $2 + 10$ coefficients (where I_o, I_e denotes these triangles and boxes):

$$A_6^{(1)} = A_6 \sum_{i=1}^{10} \text{co}_i^{(1)} I_o_i^{(1)} + A_6^s \sum_{i=1}^2 \text{ce}_i^{(1)} I_e_i^{(1)}. \quad (3.19)$$

At $L = 2$, the numerator may contain both x_{ij}^2 and the contraction of two ϵ tensor $\epsilon(a, i, j, k, *)\epsilon(b, l, m, n, *)$. As pointed out in [41], the most general topology can be taken to be double-box integrals. Topologies such as penta-box can be reduced to double-box integrals. Imposing the correct dual conformal weight yields 739 planar connected DCI integrands, subject to 54 linear relations from (2.3), leaving an ansatz with 685 coefficients:

$$I^{(2)} = \sum_{i=1}^{685} \text{ce}_i^{(2)} I_e_i^{(2)} \quad (3.20)$$

After imposing cyclic and reflection symmetry (3.13), the one-loop ansatz contains $5 = 2 + 3$ free parameters, while the two-loop ansatz contains 135 parameters. Matching against the bipartite f -graph data further reduces the numbers, but still leaves a two-dimensional ambiguity. Instead of following the strategy of [37], which would require accessing 10-point f -graph data and thus performing computation at $L = 3, 4$ in ABJM theory, we instead make use of the soft cut [42, 52], which acts as a recursion relation for the loop integrand and thus reduces the ansatz space

$$A_n^{(L)} \Big|_{x_{ai-1}^2 = x_{ai}^2 = x_{ai+1}^2 = 0} = (-1)^i A_n^{(L-1)}. \quad (3.21)$$

By using soft cut, we observed that the two remaining parameters are fixed. For example, the one-loop part can be written as follows

$$\begin{aligned} I_s^{(1)} &= \delta_1 \text{tri}[1, 3, 5] + \delta_2 \text{tri}[2, 4, 5] \\ I^{(1)} &= 2 (\text{box}[1, 3, 4, 5] + \text{box}[1, 4, 5, 6] - \text{box}[1, 2, 3, 4] - \text{box}[1, 2, 4, 6]) \\ &\quad + \beta (2\text{box}[1, 2, 4, 6] + \text{box}[1, 3, 5, 6] + \text{box}[1, 2, 3, 5] \\ &\quad - \text{box}[1, 2, 3, 6] - \text{box}[1, 2, 4, 5] - \text{box}[1, 2, 5, 6] - \text{box}[1, 3, 4, 6]), \end{aligned} \quad (3.22)$$

where the remained coefficients $\beta, \delta_1, \delta_2$ satisfies following quadratic equations

$$\begin{cases} 4(\beta - 1)^2 = \delta_1^2 + 8 \\ \delta_1^2 = \delta_2^2, \delta_1 \delta_2 = 4 \end{cases}. \quad (3.23)$$

This system admits 8 solutions, *i.e.*

$$(\beta, \delta_1, \delta_2) = (0, \pm 2i, \mp 2i), (2, \pm 2i, \mp 2i), (1 + \sqrt{3}, \pm 2, \pm 2), (1 - \sqrt{3}, \pm 2, \pm 2). \quad (3.24)$$

The first solution, $(\beta, \delta_1, \delta_2) = 2i(0, 1, -1)$, reproduces the correct one-loop integrand of [52]. Moreover, once this one-loop choice is fixed, the two-loop result automatically matches the parity-even part obtained in [52] and can be obtained via the Mathematica file. In this sense, the ambiguity is purely a one-loop effect and can be fixed once and for all at the one-loop level. Our results provide evidence for the following conjecture: the parity even part of $A_6^{(L)}$ *i.e.* $I^{(L)}$ and the entire $(L-1)$ -loop data can be extracted from $M_6^{(L)}$ up to a choice of solution to a quadratic system.

We also comment on the log of the six-point amplitude. We can define

$$\begin{aligned}\log I &= \sum_{L=0}^{\infty} a^L (\log I)^{(L)} \\ \log I_s &= \sum_{L=0}^{\infty} a^L (\log I_s)^{(L)}.\end{aligned}\tag{3.25}$$

At two-loop, (1.4) implies $M_6^{(2)} = \frac{1}{2}(\log I)^{(2)} + \frac{1}{4}((\log I_s)^{(1)})^2$. After subtracting the $I_s^{(1)}$ contribution, we obtain the two-loop logarithm of the parity-even integrand,

$$(\log I)^{(2)} = \sum_{i=1}^6 [i, i+2 | i+1, i+3] + [13|46] + [35|62] + [51|24] + ([135|24] + 5\text{cyclic}) + [135|246].\tag{3.26}$$

Here, the building blocks with bipartite pole structures are

$$[ij|kl] = 2 \frac{x_{ij}^2 x_{kl}^2 - 2x_{ik}^2 x_{jl}^2}{x_{7i}^2 x_{7j}^2 x_{8k}^2 x_{8l}^2 x_{78}^2} + 7 \leftrightarrow 8\tag{3.27}$$

$$[ijk|lm] = 2 \frac{x_{7l}^2 x_{im}^2 x_{jk}^2 + \text{cyclic}(i, j, k) + l \leftrightarrow m}{x_{7i}^2 x_{7j}^2 x_{7k}^2 x_{8l}^2 x_{8m}^2 x_{78}^2} + 7 \leftrightarrow 8$$

$$[135|246] = 2 \frac{x_{18}^2 x_{47}^2 x_{25}^2 x_{36}^2 + x_{38}^2 x_{67}^2 x_{14}^2 x_{25}^2 + x_{58}^2 x_{27}^2 x_{14}^2 x_{36}^2 + x_{78}^2 P_6}{x_{71}^2 x_{73}^2 x_{75}^2 x_{82}^2 x_{84}^2 x_{86}^2 x_{78}^2} + 7 \leftrightarrow 8,\tag{3.28}$$

where $P_6 = 4(1 \cdot 3 \cdot 5)(2 \cdot 4 \cdot 6) + x_{13}^2 x_{25}^2 x_{46}^2 + x_{13}^2 x_{25}^2 x_{46}^2 + x_{15}^2 x_{24}^2 x_{36}^2 - 2x_{14}^2 x_{25}^2 x_{36}^2$.

4 Eight-point ABJM amplitudes from f -graphs

At eight points, we focus on the extraction of the tree amplitude, which provides a more nontrivial example compared to the six-point tree-level case. We consider all codimension-1 cells defined by imposing $M_i = 0$ for $i = 1, 2, 3, 4$. Among these four cells, only three are linearly independent. Apart from the positive/negative branches, each branch now contains two solutions. Our ansatz for the tree amplitude is therefore

$$A_8 = \sum_{i=1}^3 \alpha_i \sum_{\pm} \sum_{\text{sol}} \text{LS}_{\pm, \text{sol}}[\sigma_i],\tag{4.1}$$

where σ_i denotes the cell where $M_i = 0$ and the corresponding leading singularity is given in [42]. When squaring the ansatz, in addition to the fact that $\text{LS}_{\pm, \text{sol}}[\sigma_i]^2 = 0$, we also checked numerically that

$$\text{LS}_{+, \text{sol}}[\sigma_i] \star \text{LS}_{-, \text{sol}}[\sigma_j] = 0,\tag{4.2}$$

where σ_i and σ_j denote two cells(not necessarily distinct). As follows from (3.3), this vanishing occurs because $\hat{C} \cdot \hat{C}'^T$ is not a full-rank matrix. Recall in the six-point case, only the product between the positive and negative branches gives a non-vanishing contribution to the squared amplitude. Interestingly, this vanishing pattern alternates with k . We have checked this alternating behavior numerically up to ten points. More precisely, besides the trivial vanishing $\text{LS}_{\pm, \text{sol}}[\sigma_i]^2 = 0$, we find the following systematic pattern:

$$\begin{aligned} \text{LS}_{+, \text{sol}}[\sigma_i] \star \text{LS}_{-, \text{sol}'}[\sigma_j] &= 0, \quad k \text{ even} \\ \text{LS}_{+, \text{sol}}[\sigma_i] \star \text{LS}_{+, \text{sol}'}[\sigma_j] &= \text{LS}_{-, \text{sol}}[\sigma_i] \star \text{LS}_{-, \text{sol}'}[\sigma_j] = 0, \quad k \text{ odd.} \end{aligned} \quad (4.3)$$

We leave the general proof in the Appendix B.

From (4.2), we can see that after summing over branches and solutions, the square of any cell and the product of two cells become

$$\begin{aligned} \frac{1}{2} \text{LS}[\sigma_i]^2 &= \frac{1}{2} \left(\sum_{\pm} \sum_{\text{sol}} \text{LS}_{\pm, \text{sol}}[\sigma_i] \right)^2 = \text{LS}_{+, \text{sol}_1}[\sigma_i] \star \text{LS}_{+, \text{sol}_2}[\sigma_i] + (+ \leftrightarrow -) \\ \frac{1}{2} \text{LS}[\sigma_i] \star \text{LS}[\sigma_j] &= \sum_{\text{sol}} \text{LS}_{+, \text{sol}}[\sigma_i] \star \sum_{\text{sol}'} \text{LS}_{+, \text{sol}'}[\sigma_j] + (+ \leftrightarrow -) \end{aligned} \quad (4.4)$$

On the other hand, after taking the lightlike limit of the eight-point bipartite f -graphs

$$F_8 = \text{[Diagram 1]} - 4 \text{[Diagram 2]} + 2 \text{[Diagram 3]}, \quad (4.5)$$

we obtain the eight-point squared tree amplitude

$$\begin{aligned} M_8^{(0)} &= \frac{2}{x_{14}^2 x_{36}^2 x_{58}^2 x_{72}^2} \left(-2 + \frac{1}{v_2} + \frac{1}{v_4} + u_1 v_1 u_6 + u_3 v_3 u_8 + u_4 u_7 v_3 + u_2 u_5 v_1 + \frac{(u_1 + u_5)v_1}{v_2} + \frac{(u_3 + u_7)v_3}{v_4} \right) \\ &+ \frac{2}{x_{25}^2 x_{47}^2 x_{61}^2 x_{83}^2} \left(-2 + \frac{1}{v_1} + \frac{1}{v_3} + u_2 v_2 u_7 + u_4 v_4 u_1 + u_5 u_8 v_4 + u_3 u_6 v_2 + \frac{(u_4 + u_8)v_4}{v_1} + \frac{(u_2 + u_6)v_2}{v_3} \right), \end{aligned} \quad (4.6)$$

where the cross ratios are defined [42] as $u_i = \frac{x_{ii+1}^2 x_{i+3, i+7}^2}{x_{ii+3}^2 x_{i+2, i+7}^2}$, $v_i = \frac{x_{ii+3}^2 x_{i+4, i+7}^2}{x_{ii+4}^2 x_{i+3, i+7}^2}$.

By numerically comparing the squared ansatz and the squared amplitude from the f -graph, we obtained

$$\alpha_1 = \alpha_3 = \pm 1, \alpha_2 = 0, \quad (4.7)$$

and hence

$$A_8 = \pm \left(\sum_{\pm} \sum_{\text{sol}} \text{LS}_{\pm, \text{sol}}[\sigma_1] + \sum_{\pm} \sum_{\text{sol}} \text{LS}_{\pm, \text{sol}}[\sigma_3] \right). \quad (4.8)$$

By choosing the positive sign, we reproduce the result in [8, 42]. We note that the cyclic-by-two symmetry, although not imposed at tree level, emerges manifestly in the final result.

5 Discussions and Outlook

The hidden permutation symmetry of squared amplitudes provides a new way for studying ABJM amplitudes and reveals remarkable unification and simplifications: different cross-sections with fixed $n+L$ are combined in a single function, F_N , which is a linear combination of bipartite f -graphs (they can also be rewritten using planar f -graphs via Gram identities). In this paper, we provide some evidence for the conjecture that individual amplitudes can be extracted from these squared ones. As a proof of concept, by constructing an ansatz via squaring leading singularities (or Yangian invariants), we show how to extract from F_N with $N \leq 8$ the six-particle amplitudes at tree-level, one-loop, and (the parity-even part of) two-loop case, as well as eight-point tree amplitudes. Moreover, the four-point case is similar to the $n = 5$ case for SYM, and we extract up to $L = 6$ results from F_{10} : not only have we obtained a new planar representation for five-loop integrands directly, but we have also been able to provide new results for the log of four-point amplitudes at six loops!

This work is a small step in the broader program of exploring the hidden permutation symmetry of ABJM squared amplitudes and possible relations with other quantities such as correlators and Wilson loops, as well as underlying positive geometries such as the ABJM amplituhedron [16, 18, 19, 53–57]. For four points, it would be interesting to reorganize the entire logarithm of the amplitude in terms of bipartite negative geometries and fix the canonical forms for such geometries with different “topologies”. An important physical application of such integrands is that by integrating them we can extract the important quantity known as the cusp anomalous dimensions [58–61], and how to do this at $L = 6$ remains an important open problem. It would also be highly desirable to understand how vanishing cuts in loop sub-topologies connect to the conjecture [60] that loop topologies do not contribute to Γ_{cusp} . Along the same line, it would also be very interesting to study periods of these weight-3 f -graphs and their relations with certain “integrated correlators” similar to the SYM case [62–66], and integrations for higher-point amplitudes in ABJM theory.

Another intriguing direction is to study the squared amplituhedron and correlahedron in $D = 3$ via dimension reduction of their four-dimensional counterparts [44, 67–69]. While it works nicely for the amplituhedra, directly reducing the correlahedron in $D = 4$ by flipping all signs except for $\Delta^2 > 0$ does not seem to work: the one-loop object does not vanish, and it produces a two-loop correlator in (1.9) with additional kissing-triangles as the “chamber form”. Despite these discouraging results, it produces correct lightlike limits, *i.e.* vanishes at four-point one loop as well as five-point tree-level and also gives correct squared amplitude at four-point two-loop and six-point tree-level. Moreover, the geometry after taking the lightlike limit can be directly defined: the four-point squared ABJM amplituhedron in momentum twistor space can be defined as

$$\langle 1234 \rangle < 0, \frac{\langle A_j B_j 12 \rangle}{\langle A_j B_j 41 \rangle} < 0, \frac{\langle A_j B_j 23 \rangle}{\langle A_j B_j 41 \rangle} < 0, \frac{\langle A_j B_j 34 \rangle}{\langle A_j B_j 41 \rangle} < 0, \frac{\langle A_i B_i A_j B_j \rangle}{\langle A_i B_i 41 \rangle \langle A_j B_j 41 \rangle} < 0 \quad (5.1)$$

with $A_i \cdot \Omega \cdot B_i = 0$, $i, j = 1, 2, \dots, L$.

and summing over all 2^L sign choices reproduces exactly the combination appearing in (1.4)

at all loop orders. We leave deeper exploration for future work.

For $n \geq 8$ cases, it is already interesting to study tree-level amplitudes from the f -graphs, where (3.3) provides a powerful tool. Regarding this, we point out that the determinant formula is general and it would be interesting to apply it to other theories, such as squaring super-amplitudes in SYM and supergravity in four dimensions [70]. Moreover, while our computation in this paper is formulated in spinor-helicity variables, it would also be very interesting to extend this determinant formula to momentum twistor space [9, 19, 71, 72], where (super)momentum conservation is manifest. Such an extension could be crucial for a better understanding of underlying positive geometries, including the ABJM amplituhedra in both spaces, the square of such objects and analogous “correlahedron” as their off-shell generalizations.

Last but not least, it would be extremely interesting if our study could shed more lights into the origin of this hidden permutation symmetry, and the longstanding problem of amplitude/Wilson loop/correlator triality in ABJM theory.

Acknowledgments

It is our pleasure to thank Chia-Kai Kuo, Xichen Li, Canxin Shi and Yichao Tang for helpful discussions and/or collaborations on related topics. SH has been supported by the National Natural Science Foundation of China under Grant No. 12225510, 12447101, 12247103, and by the New Cornerstone Science Foundation. YZ was also supported in part by the Deutsche Forschungsgemeinschaft (DFG, German Research Foundation) Projektnummer 508889767/FOR5582 “Modern Foundations of Scattering Amplitudes” .

A The definition of three-loop planar DCI integrands

Here we present the definition of DCI integrals at $L = 3$ extracted from the planar f -graph in ABJM theory. All the x_{13}^2, x_{24}^2 are omitted and those valency-4 vertices i has a numerator ϵ_i . The entire integrand is also included in the ancillary file.

$$\begin{aligned}
 \begin{array}{c} \text{Diagram 1} \\ \text{Diagram 2} \end{array} &= \frac{\epsilon_5}{x_{1,5}^2 x_{1,6}^2 x_{1,7}^2 x_{2,7}^2 x_{3,5}^2 x_{3,6}^2 x_{3,7}^2 x_{4,5}^2 x_{5,6}^2}, & \begin{array}{c} \text{Diagram 3} \\ \text{Diagram 4} \end{array} &= \frac{\epsilon_5}{x_{1,5}^2 x_{1,6}^2 x_{1,7}^2 x_{3,5}^2 x_{3,6}^2 x_{3,7}^2 x_{5,6}^2 x_{5,7}^2} \\
 \begin{array}{c} \text{Diagram 5} \\ \text{Diagram 6} \end{array} &= \frac{\epsilon_6 x_{2,5}^2}{x_{1,5}^2 x_{1,6}^2 x_{1,7}^2 x_{2,6}^2 x_{3,5}^2 x_{3,6}^2 x_{3,7}^2 x_{5,6}^2 x_{5,7}^2}, & \begin{array}{c} \text{Diagram 7} \\ \text{Diagram 8} \end{array} &= \frac{\epsilon_5 x_{2,5}^2}{x_{1,5}^2 x_{1,7}^2 x_{2,6}^2 x_{2,7}^2 x_{3,5}^2 x_{3,6}^2 x_{4,5}^2 x_{5,6}^2 x_{5,7}^2} \\
 \begin{array}{c} \text{Diagram 9} \\ \text{Diagram 10} \end{array} &= \frac{\epsilon_5}{x_{1,5}^2 x_{1,7}^2 x_{2,7}^2 x_{3,5}^2 x_{3,6}^2 x_{4,6}^2 x_{5,6}^2 x_{5,7}^2}, & \begin{array}{c} \text{Diagram 11} \\ \text{Diagram 12} \end{array} &= \frac{\epsilon_6}{x_{1,6}^2 x_{1,7}^2 x_{2,7}^2 x_{3,5}^2 x_{3,6}^2 x_{4,6}^2 x_{5,6}^2 x_{5,7}^2}
 \end{aligned}$$

$$\begin{aligned}
& \text{Diagram 1} = \frac{\epsilon_7 x_{2,6}^2 x_{4,5}^2}{x_{1,5}^2 x_{1,6}^2 x_{1,7}^2 x_{2,7}^2 x_{3,5}^2 x_{3,6}^2 x_{3,7}^2 x_{4,6}^2 x_{5,6}^2 x_{5,7}^2}, & \text{Diagram 2} = \frac{\epsilon_5 x_{1,7}^2 x_{3,6}^2}{x_{1,6}^2 x_{2,5}^2 x_{2,6}^2 x_{2,7}^2 x_{3,7}^2 x_{4,5}^2 x_{4,6}^2 x_{4,7}^2 x_{5,6}^2 x_{5,7}^2} \\
& \text{Diagram 3} = \frac{\epsilon_5 x_{1,5}^2}{x_{1,6}^2 x_{1,7}^2 x_{2,5}^2 x_{3,5}^2 x_{4,5}^2 x_{5,6}^2 x_{5,7}^2 x_{6,7}^2}, & \text{Diagram 4} = \frac{\epsilon_5}{x_{1,7}^2 x_{2,6}^2 x_{3,5}^2 x_{4,5}^2 x_{5,6}^2 x_{5,7}^2 x_{6,7}^2} \\
& \text{Diagram 5} = \frac{\epsilon_6 x_{1,5}^2}{x_{1,6}^2 x_{1,7}^2 x_{2,6}^2 x_{3,5}^2 x_{4,5}^2 x_{5,6}^2 x_{5,7}^2 x_{6,7}^2}, & \text{Diagram 6} = \frac{\epsilon_5 x_{1,7}^2 x_{2,5}^2 x_{3,6}^2}{x_{1,5}^2 x_{1,6}^2 x_{2,6}^2 x_{2,7}^2 x_{3,5}^2 x_{3,7}^2 x_{4,5}^2 x_{5,6}^2 x_{5,7}^2 x_{6,7}^2} \\
& \text{Diagram 7} = \frac{\epsilon_7 x_{5,6}^2}{x_{1,5}^2 x_{1,6}^2 x_{1,7}^2 x_{2,6}^2 x_{3,5}^2 x_{3,6}^2 x_{3,7}^2 x_{4,5}^2 x_{5,7}^2 x_{6,7}^2}
\end{aligned}$$

B Proof of Theorem (4.3)

Let $V = \hat{C}'|_{\text{sol}}$ and $W = \hat{C}'|_{\text{sol}'}$, with branch signs $\sigma(V), \sigma(W) \in \{\pm 1\}$. The row vectors of V and W are denoted by v_i and w_j ($i, j = 1, \dots, k$). We define a $k \times k$ matrix P by

$$P := V \eta W^T, \quad P_{ij} = (-1)^j v_i w_j^T. \quad (\text{B.1})$$

We shall prove that, for $V \neq W$,

$$\sigma(V)\sigma(W) = (-1)^{k+1} \Rightarrow \det P = 0. \quad (\text{B.2})$$

Proof. We begin by permuting the columns of V and W by an invertible permutation matrix P_π so that

$$\eta' := P_\pi^T \eta P_\pi = \text{diag}(\underbrace{1, \dots, 1}_k, \underbrace{-1, \dots, -1}_k). \quad (\text{B.3})$$

Define $V' := V P_\pi$ and $W' := W P_\pi$. Since P_π is invertible, V' and W' are also elements of the orthogonal Grassmannian $OG(k, 2k)$ with respect to the metric η' , and their branch are unchanged.

Using the $GL(k)$ gauge-fixing, we may further bring V' and W' to the standard forms

$$V' = [I_k \ C], \quad W' = [I_k \ D], \quad (\text{B.4})$$

where $C, D \in O(k)$ are orthogonal matrices. In this parametrization, the branch signs are given by

$$\sigma(V) = \det C, \quad \sigma(W) = \det D. \quad (\text{B.5})$$

The matrix P is similar to P'

$$P \sim P' = V' \eta' W'^T = (I_k - CD^T) \quad (\text{B.6})$$

Taking determinants yields

$$\det P = \det P' = \det(I_k - CD^T) \equiv \det(I_k - Q), \quad (\text{B.7})$$

where we have defined $Q := CD^T \in O(k)$. Therefore, P is full rank if and only if $\det(I_k - Q) \neq 0$. Since Q is an orthogonal matrix,

$$\det(I_k - Q) = \det(Q) \det(Q^T - I_k) = (-1)^k \det(Q) \det(I_k - Q). \quad (\text{B.8})$$

It follows that

$$(1 - (-1)^k \det Q) \det(I_k - Q) = 0. \quad (\text{B.9})$$

Hence if

$$\det Q = (-1)^{k+1} \neq (-1)^k, \quad (\text{B.10})$$

$\det(I_k - Q)$ must vanish.

Finally, using $\det Q = \det C \det D = \sigma(V)\sigma(W)$, we conclude that

$$\sigma(V)\sigma(W) = (-1)^{k+1} \Rightarrow \det P = 0.$$

Equivalently, when k is even, products between different branches will vanish, while at odd k , products between the same branches vanish. □

References

- [1] O. Aharony, O. Bergman, D. L. Jafferis, and J. Maldacena, *$\mathcal{N}=6$ Superconformal Chern-Simons-Matter Theories, M2-Branes and Their Gravity Duals*, *JHEP* **0810** (2008) 091, [[arXiv:0806.1218](#)].
- [2] K. Hosomichi, K.-M. Lee, S. Lee, S. Lee, and J. Park, *$N=5,6$ Superconformal Chern-Simons Theories and M2-branes on Orbifolds*, *JHEP* **09** (2008) 002, [[arXiv:0806.4977](#)].
- [3] J. M. Drummond, J. Henn, G. P. Korchemsky, and E. Sokatchev, *Dual superconformal symmetry of scattering amplitudes in $N=4$ super-Yang-Mills theory*, *Nucl. Phys. B* **828** (2010) 317–374, [[arXiv:0807.1095](#)].
- [4] A. Brandhuber, P. Heslop, and G. Travaglini, *A Note on dual superconformal symmetry of the $N=4$ super Yang-Mills S-matrix*, *Phys. Rev. D* **78** (2008) 125005, [[arXiv:0807.4097](#)].
- [5] J. M. Drummond, J. M. Henn, and J. Plefka, *Yangian Symmetry of Scattering Amplitudes in $\mathcal{N}=4$ super Yang-Mills Theory*, *JHEP* **05** (2009) 046, [[arXiv:0902.2987](#)].
- [6] T. Bargheer, F. Loebbert, and C. Meneghelli, *Symmetries of Tree-Level Scattering Amplitudes in $\mathcal{N}=6$ Superconformal Chern-Simons Theory*, *Phys. Rev.* **D82** (2010) 045016, [[arXiv:1003.6120](#)].
- [7] Y.-t. Huang and A. E. Lipstein, *Dual Superconformal Symmetry of $N=6$ Chern-Simons Theory*, *JHEP* **11** (2010) 076, [[arXiv:1008.0041](#)].
- [8] D. Gang, Y.-t. Huang, E. Koh, S. Lee, and A. E. Lipstein, *Tree-level Recursion Relation and Dual Superconformal Symmetry of the ABJM Theory*, *JHEP* **03** (2011) 116, [[arXiv:1012.5032](#)].

- [9] N. Arkani-Hamed, J. L. Bourjaily, F. Cachazo, A. B. Goncharov, A. Postnikov, and J. Trnka, *Grassmannian Geometry of Scattering Amplitudes*. Cambridge University Press, 4, 2016.
- [10] S. Lee, *Yangian Invariant Scattering Amplitudes in Supersymmetric Chern-Simons Theory*, *Phys. Rev. Lett.* **105** (2010) 151603, [[arXiv:1007.4772](#)].
- [11] Y.-T. Huang and C. Wen, *ABJM Amplitudes and the Positive Orthogonal Grassmannian*, *JHEP* **1402** (2014) 104, [[arXiv:1309.3252](#)].
- [12] Y.-t. Huang, C. Wen, and D. Xie, *The Positive Orthogonal Grassmannian and Loop Amplitudes of ABJM*, *J. Phys.* **A47** (2014), no. 47 474008, [[arXiv:1402.1479](#)].
- [13] N. Arkani-Hamed and J. Trnka, *The Amplituhedron*, *JHEP* **10** (2014) 030, [[arXiv:1312.2007](#)].
- [14] N. Arkani-Hamed, J. Henn, and J. Trnka, *Nonperturbative negative geometries: amplitudes at strong coupling and the amplituhedron*, *JHEP* **03** (2022) 108, [[arXiv:2112.06956](#)].
- [15] D. Damgaard, L. Ferro, T. Lukowski, and M. Parisi, *The Momentum Amplituhedron*, *JHEP* **08** (2019) 042, [[arXiv:1905.04216](#)].
- [16] S. He, C.-K. Kuo, and Y.-Q. Zhang, *The momentum amplituhedron of SYM and ABJM from twistor-string maps*, *JHEP* **02** (2022) 148, [[arXiv:2111.02576](#)].
- [17] Y.-t. Huang, R. Kojima, C. Wen, and S.-Q. Zhang, *The orthogonal momentum amplituhedron and ABJM amplitudes*, *JHEP* **01** (2022) 141, [[arXiv:2111.03037](#)].
- [18] S. He, C.-K. Kuo, Z. Li, and Y.-Q. Zhang, *All-Loop Four-Point Aharony-Bergman-Jafferis-Maldacena Amplitudes from Dimensional Reduction of the Amplituhedron*, *Phys. Rev. Lett.* **129** (2022), no. 22 221604.
- [19] S. He, Y.-t. Huang, and C.-K. Kuo, *The ABJM Amplituhedron*, *JHEP* **09** (2023) 165, [[arXiv:2306.00951](#)]. [Erratum: *JHEP* 04, 064 (2024)].
- [20] S. Caron-Huot, *Notes on the scattering amplitude / Wilson loop duality*, *JHEP* **07** (2011) 058, [[arXiv:1010.1167](#)].
- [21] L. F. Alday, B. Eden, G. P. Korchemsky, J. Maldacena, and E. Sokatchev, *From correlation functions to Wilson loops*, *JHEP* **09** (2011) 123, [[arXiv:1007.3243](#)].
- [22] B. Eden, P. Heslop, G. P. Korchemsky, and E. Sokatchev, *The super-correlator/super-amplitude duality: Part I*, *Nucl. Phys. B* **869** (2013) 329–377, [[arXiv:1103.3714](#)].
- [23] B. Eden, P. Heslop, G. P. Korchemsky, and E. Sokatchev, *The super-correlator/super-amplitude duality: Part II*, *Nucl. Phys. B* **869** (2013) 378–416, [[arXiv:1103.4353](#)].
- [24] P. Heslop, *The SAGEX Review on Scattering Amplitudes, Chapter 8: Half BPS correlators*, *J. Phys. A* **55** (2022), no. 44 443009, [[arXiv:2203.13019](#)].
- [25] J. M. Henn, J. Plefka, and K. Wiegandt, *Light-like polygonal Wilson loops in 3d Chern-Simons and ABJM theory*, *JHEP* **08** (2010) 032, [[arXiv:1004.0226](#)]. [Erratum: *JHEP* 11, 053 (2011)].
- [26] M. S. Bianchi, M. Leoni, A. Mauri, S. Penati, C. Ratti, and A. Santambrogio, *From Correlators to Wilson Loops in Chern-Simons Matter Theories*, *JHEP* **06** (2011) 118, [[arXiv:1103.3675](#)].

- [27] M. S. Bianchi, M. Leoni, A. Mauri, S. Penati, and A. Santambrogio, *Scattering Amplitudes/Wilson Loop Duality In ABJM Theory*, *JHEP* **01** (2012) 056, [[arXiv:1107.3139](#)].
- [28] T. Bargheer, N. Beisert, F. Loebbert, and T. McLoughlin, *Conformal Anomaly for Amplitudes in $\mathcal{N} = 6$ Superconformal Chern-Simons Theory*, *J. Phys. A* **45** (2012) 475402, [[arXiv:1204.4406](#)].
- [29] M. Rosso and C. Vergu, *Wilson loops in $N=6$ superspace for ABJM theory*, *JHEP* **06** (2014) 176, [[arXiv:1403.2336](#)].
- [30] N. Berkovits and J. Maldacena, *Fermionic T-Duality, Dual Superconformal Symmetry, and the Amplitude/Wilson Loop Connection*, *JHEP* **09** (2008) 062, [[arXiv:0807.3196](#)].
- [31] E. Ó. Colgáin and A. Pittelli, *A Requiem for $AdS_4 \times CP^3$ Fermionic self-T-duality*, *Phys. Rev. D* **94** (2016), no. 10 106006, [[arXiv:1609.03254](#)].
- [32] S. He, C. Shi, Y. Tang, and Y.-Q. Zhang, *A Hidden Permutation Symmetry of Squared Amplitudes in ABJM Theory*, [arXiv:2508.03813](#).
- [33] J. L. Bourjaily, P. Heslop, and V.-V. Tran, *Amplitudes and Correlators to Ten Loops Using Simple, Graphical Bootstraps*, *JHEP* **11** (2016) 125, [[arXiv:1609.00007](#)].
- [34] S. He, C. Shi, Y. Tang, and Y.-Q. Zhang, *The Cusp Limit of Correlators and A New Graphical Bootstrap for Correlators/Amplitudes to Eleven Loops*, [arXiv:2410.09859](#).
- [35] J. L. Bourjaily, S. He, C. Shi, and Y. Tang, *The Four-Point Correlator of Planar sYM at Twelve Loops*, [arXiv:2503.15593](#).
- [36] R. G. Ambrosio, B. Eden, T. Goddard, P. Heslop, and C. Taylor, *Local integrands for the five-point amplitude in planar $N=4$ SYM up to five loops*, *JHEP* **01** (2015) 116, [[arXiv:1312.1163](#)].
- [37] P. Heslop and V.-V. Tran, *Multi-particle amplitudes from the four-point correlator in planar $\mathcal{N} = 4$ SYM*, *JHEP* **07** (2018) 068, [[arXiv:1803.11491](#)].
- [38] R. Britto, F. Cachazo, and B. Feng, *Generalized Unitarity and One-Loop Amplitudes in $\mathcal{N}=4$ Super-Yang-Mills*, *Nucl. Phys.* **B725** (2005) 275–305, [[hep-th/0412103](#)].
- [39] M. S. Bianchi, M. Leoni, A. Mauri, S. Penati, and A. Santambrogio, *One Loop Amplitudes In ABJM*, *JHEP* **07** (2012) 029, [[arXiv:1204.4407](#)].
- [40] A. Brandhuber, G. Travaglini, and C. Wen, *A note on amplitudes in $N=6$ superconformal Chern-Simons theory*, *JHEP* **07** (2012) 160, [[arXiv:1205.6705](#)].
- [41] S. Caron-Huot and Y.-t. Huang, *The two-loop six-point amplitude in ABJM theory*, *JHEP* **03** (2013) 075, [[arXiv:1210.4226](#)].
- [42] S. He, Y.-t. Huang, C.-K. Kuo, and Z. Li, *The two-loop eight-point amplitude in ABJM theory*, *JHEP* **02** (2023) 065, [[arXiv:2211.01792](#)].
- [43] H. Elvang and Y.-t. Huang, *Scattering Amplitudes*, [arXiv:1308.1697](#).
- [44] G. Dian and P. Heslop, *Amplituhedron-like geometries*, *JHEP* **11** (2021) 074, [[arXiv:2106.09372](#)].
- [45] S. He, X. Jiang, Q. Yang, and Y.-Q. Zhang, “From squared amplitudes to energy correlators.” 8, 2024.

- [46] S. He, X. Li, J. Lin, J. Liu, and K. Yan, *Bootstrapping form factor squared in $\mathcal{N} = 4$ super-Yang-Mills*, [arXiv:2506.07796](#).
- [47] B. Eden, P. Heslop, G. P. Korchemsky, and E. Sokatchev, *Hidden symmetry of four-point correlation functions and amplitudes in $N=4$ SYM*, *Nucl. Phys. B* **862** (2012) 193–231, [[arXiv:1108.3557](#)].
- [48] S. He and Y. Tang, *Algorithm for symbol integrations for loop integrals*, *Phys. Rev. D* **108** (2023), no. 4 L041702, [[arXiv:2304.01776](#)].
- [49] W.-M. Chen and Y.-t. Huang, *Dualities for Loop Amplitudes of $N=6$ Chern-Simons Matter Theory*, *JHEP* **11** (2011) 057, [[arXiv:1107.2710](#)].
- [50] B. Eden, P. Heslop, G. P. Korchemsky, and E. Sokatchev, *Constructing the Correlation Function of Four Stress-Tensor Multiplets and the Four-Particle Amplitude in $\mathcal{N} = 4$ SYM*, *Nucl. Phys.* **B862** (2012) 450–503, [[arXiv:1201.5329](#)].
- [51] M. S. Bianchi and M. Leoni, *On the ABJM four-point amplitude at three loops and BDS exponentiation*, *JHEP* **11** (2014) 077, [[arXiv:1403.3398](#)].
- [52] S. Caron-Huot and Y.-t. Huang, *The Two-Loop Six-Point Amplitude in ABJM Theory*, *JHEP* **1303** (2013) 075, [[arXiv:1210.4226](#)].
- [53] Y.-T. Huang, R. Kojima, C. Wen, and S.-Q. Zhang, *The orthogonal momentum amplituhedron and ABJM amplitudes*, *JHEP* **01** (2022) 141, [[arXiv:2111.03037](#)].
- [54] T. Lukowski, R. Moerman, and J. Stalknecht, *On the geometry of the orthogonal momentum amplituhedron*, [arXiv:2112.03294](#).
- [55] M. Oren-Perstein and R. Tessler, *The BCFW Tiling of the ABJM Amplituhedron*, [arXiv:2501.07576](#).
- [56] T. Lukowski and J. Stalknecht, *Momentum Amplituhedron for $N=6$ Chern-Simons-Matter Theory: Scattering Amplitudes from Configurations of Points in Minkowski Space*, *Phys. Rev. Lett.* **131** (2023), no. 16 161601, [[arXiv:2306.07312](#)].
- [57] L. Ferro, R. Glew, T. Lukowski, and J. Stalknecht, *The Geometry of BCFW for ABJM Loop Integrands*, [arXiv:2510.25733](#).
- [58] S. He, C.-K. Kuo, Z. Li, and Y.-Q. Zhang, *Emergent unitarity, all-loop cuts and integrations from the ABJM amplituhedron*, *JHEP* **07** (2023) 212, [[arXiv:2303.03035](#)].
- [59] J. M. Henn, M. Lagares, and S.-Q. Zhang, *Integrated negative geometries in ABJM*, [arXiv:2303.02996](#).
- [60] Z. Li, *Integrating the full four-loop negative geometries and all-loop ladder-type negative geometries in ABJM theory*, *JHEP* **10** (2024) 124, [[arXiv:2402.17023](#)].
- [61] M. Lagares and S.-Q. Zhang, *Higher-loop integrated negative geometries in ABJM*, *JHEP* **05** (2024) 142, [[arXiv:2402.17432](#)].
- [62] C. Wen and S.-Q. Zhang, *Integrated correlators in $\mathcal{N} = 4$ super Yang-Mills and periods*, *JHEP* **05** (2022) 126, [[arXiv:2203.01890](#)].
- [63] A. Brown, P. Heslop, C. Wen, and H. Xie, *Integrated correlators in $\mathcal{N} = 4$ SYM beyond localisation*, *Phys. Rev. Lett.* **132** (2024), no. 10 101602, [[arXiv:2308.07219](#)].
- [64] S.-Q. Zhang, *Nonplanar integrated correlator in $N=4$ SYM*, *Phys. Rev. D* **110** (2024), no. 2 025003, [[arXiv:2404.18900](#)].

- [65] S. He, X. Jiang, J. Liu, and Y.-Q. Zhang, *Notes on Conformal Integrals: Coulomb Branch Amplitudes, Magic Identities and Bootstrap*, [arXiv:2502.08871](#).
- [66] S. He and X. Jiang, *Solving Infinite Families of Dual Conformal Integrals and Periods*, [arXiv:2506.20095](#).
- [67] B. Eden, P. Heslop, and L. Mason, *The Correlahedron*, *JHEP* **09** (2017) 156, [[arXiv:1701.00453](#)].
- [68] S. He, Y.-t. Huang, and C.-K. Kuo, *All-loop geometry for four-point correlation functions*, *Phys. Rev. D* **110** (2024), no. 8 L081701, [[arXiv:2405.20292](#)].
- [69] S. He, Y.-t. Huang, and C.-K. Kuo, *Leading singularities and chambers of Correlahedron*, [arXiv:2505.09808](#).
- [70] D. Chicherin, G. P. Korchemsky, E. Sokatchev, and A. Zhiboedov, *Energy correlators in four-dimensional gravity*, [arXiv:2512.23791](#).
- [71] N. Arkani-Hamed, F. Cachazo, and C. Cheung, *The Grassmannian Origin Of Dual Superconformal Invariance*, *JHEP* **03** (2010) 036, [[arXiv:0909.0483](#)].
- [72] H. Elvang, Y.-t. Huang, C. Keeler, T. Lam, T. M. Olson, S. B. Roland, and D. E. Speyer, *Grassmannians for scattering amplitudes in 4d $\mathcal{N} = 4$ SYM and 3d ABJM*, *JHEP* **12** (2014) 181, [[arXiv:1410.0621](#)].